

# Spatio-temporal analysis of *b*-value prior to 28 April 2021 Assam Earthquake and implications thereof

Vickey Sharma<sup>1</sup>, Dipok K. Bora<sup>2,3</sup>, Rajib Biswas<sup>\*,1</sup>

<sup>(1)</sup> Applied Geophysics Lab, Department of Physics, Tezpur University, Tezpur-784028, India

<sup>(2)</sup> Department of Physics, Diphu Government College, Karbi Anglong-782 460, Assam, India

<sup>(3)</sup> Government Model college, Deithor, Karbi Anglong-782 480, Assam, India

Article history: received February 11, 2022; accepted June 14, 2022

## Abstract

Here, we report a Spatio-temporal analysis of the frequency magnitude distribution of earthquakes (*b*-value) before the 28<sup>th</sup> April 2021 ( $M_w$  6.4) earthquake event observed in northeast India. To estimate the average *b*-value for the study region, a data set of 750 earthquake events with magnitude  $M_w \geq 3.9$  is extracted from the homogenous part of the earthquake catalog (1950-2021) documented by the United States Geological Survey (USGS) and International seismological center (ISC) in the region. For spatial analysis of the disparities in *b*-value, the whole study region is subdivided into 16 square grids of dimension  $1^\circ \times 1^\circ$  and the *b*-value is calculated for each subsection. In congruence with other studies, this work yields *b*-values ranging from 0.66 to 1.25. After the calculation of the *b*-value for each grid, it is observed that the grid with the epicentral location of the 28<sup>th</sup> April 2021 (6.4) earthquake has a low *b*-value. Accordingly, the spatial correlation and aberrant pattern between *b*-value and focal depth have been comprehensively explored. It is observed that the *b*-value significantly dips within a depth range of  $\sim 15$ -35 km which implicates high-stress accumulation and crustal homogeneity. The depth-wise variation in *b*-value infers the antithetical relationship between *b*-value and crustal stress. Mostly interplate earthquakes are observed in the study region; thereby hinting at intense seismicity at the upper crust.

Keywords: *b*-value; Seismicity; Fault mechanisms; Stress; Seismotectonics

---

## 1. Introduction

Earthquakes are very frequent in Northeast (NE) India. During the past 100 years, this region has experienced 18 large earthquakes. The 12 June 1897 Shillong earthquake ( $M_w$  8.1) [England and Bilham, 2015] and the Assam-Tibet earthquake of 15 August 1950 ( $M_w$  8.4) [Ajanta and Farha, 2019] caused large human casualties along with severe property losses. In NE India, the Mikir hills plateau flanks two major faults namely the Bomdila fault in the east and the Kopili fault to the west. Both these faults are characterized by strike-slip kinematics. A recent study [Sharma et al., 2018] inferred that the Strike-slip fault can produce major earthquakes ( $M > 8$ ). Kopili fault and its neighboring region

which is our study region are one of the most seismically active regions of NE India and the region is bounded by latitude 24°-28°N and longitude 90°-94°E [Mahanta et al., 2012]. Roy and Purohit [2018] inferred that the Subduction of the Indian plate under the Eurasian plate causes various tectonic disturbances in this region. The seismic analysis of this region is important for a better understanding of seismic hazard assessment. The widely established frequency-magnitude distribution equation after [Gutenberg and Richter, 1944] – i.e.,  $\log_{10}N(M) = a - M$  links the cumulative number of earthquakes ( $M$ ) with magnitude  $M$  with two important coefficients, namely  $a$  and  $b$ . In this relation,  $a$  takes care of seismic activity whereas  $b$  is identified as a unique characteristic parameter intrinsic to a group of events. Suitably, geoscientists term it as the  $b$ -value parameter. Various studies have been carried out to investigate the relationship between  $b$ -value and other parameters including crustal stress, heterogeneity of earth crust, seismic moment, Bouguer gravity, and focal mechanism solution for northeast India. In a recent work, Khan and Chakraborty [2007] show the correlation between  $b$ -value and Bouguer gravity anomaly for the Shillong region, while Bhattacharya, Majumdar and Kayal [2002] show the correlation between seismic  $b$ -value and fractal dimension for entire northeast India. A similar attempt was made by Khan, Ghosh, Chakraborty, Mukherjee [2011] which evaluates the seismic  $b$ -value for entire northeast India and also assessed the stress level, and finally established a correlation between  $b$ -value and seismic moment ( $M_0$ ). Bora, Borah, Mahanta, and Borgohain [2018] show a correlation between  $b$ -value and seismic moment, focal mechanism solution, and Bouguer gravity for the IB region of northeast India in a recent paper. Similar research has been done in other seismically active places throughout the world. In recent work Mohammed Salih Al-Heety, and Mohammad, [2021] showed the reliance of  $b$ -value over focal depth and focal mechanism solution at a global level. On a similar note,  $b$ -values are linked with crustal properties as well as stress magnitudes. According to laboratory research [Kamer and Hiemer, 2015; Schorlemmer et al., 2005], seismic  $b$ -values range from 0.5 to 1.5. Furthermore, for the Tohoku (2011) and Sumatra (2004) earthquakes, Nanjo, Hirata, Obara, and Kasahara [2012] assessed the phenomena of drop-in  $b$ -value before the mainshock as an earthquake precursor. Borgohain, Borah, Biswas and Bora [2018] conducted a similar study for the Manipur (2016, 6.7) earthquake, however, they only looked at a small area and didn't look into the seismic hazard potential of the Kopili lineament. All known  $b$ -value studies for northeast India cover a vast area. Furthermore, when dealing with  $b$ -value estimation at the regional level, macroscale heterogeneities are frequently overlooked. There lies an obvious dependence of  $b$ -values along with macroscale heterogeneities as well as the allied seismicity associated with it. Considering all these into consideration, we present here a detailed study where the variation of the  $b$ -value and its reliance on focal depth in the Kopili fault and neighboring region before the 28<sup>th</sup> April 2021 Assam earthquake ( $M_w$  6.4) is highlighted. The interplate model for this region showing all the major earthquakes is also projected in this study. Starting from the estimation of the average  $b$ -value, we include the macroscale heterogeneities to formulate a correlational approach with  $b$ -value. Further, the anomalies before the  $b$ -value hitherto are also delineated. The study has been systematically ordered. First section deals with the Tectonic setup; followed by the data used in this study. Next section deals with the estimation of the  $b$ -value with ample illustrations. The results and discussions follow thereof.

## 2. Tectonic setup

The NE India as shown in Figure 1 is characterized by high seismic activity. Subduction of the Indian plate under the Eurasian plate results in complex seismicity of this region [Roy and Purohit, 2018].

The topological map of the study region is shown in Figure 2. The unabridged study area consists of three major tectonic entities with some inimitable tectonic features. The complete study region is bounded by latitude 24°-28°N and longitude 90°-94°E which mainly consists of a) the eastern Himalayan zone b) the Assam valley region c) the Shillong plateau region. The Mikir hill plateau encompassed the two most seismic active faults including the Bomdila fault and the Kopili fault. As per reports, the length of NW-SE trending KF emerges to be 300 km with 50 km width. It covers the western part of Manipur to the trijunction of Bhutan, Arunachal Pradesh, and Assam. The 2009 Bhutan earthquake has been established to be stemming from KF [Kayal, Bora, et al., 2010]. There is evidence of active seismicity in the KF region with further expansion towards MCT in the Bhutan Himalaya. Meanwhile, higher activity is observed in Kopili Fault at the junction of MBT and MCT. The August 19, 2009 earthquake bears testimony to this with the further occurrence of the 21st September 2009 earthquake whose epicenter lied at the northern juncture of the Kopili Fault with MCT. As per reports, both these seismic occurrences are typified as shallow focus with faulting of right-lateral strike-slip nature. This can be envisaged as an ongoing compressional stage for

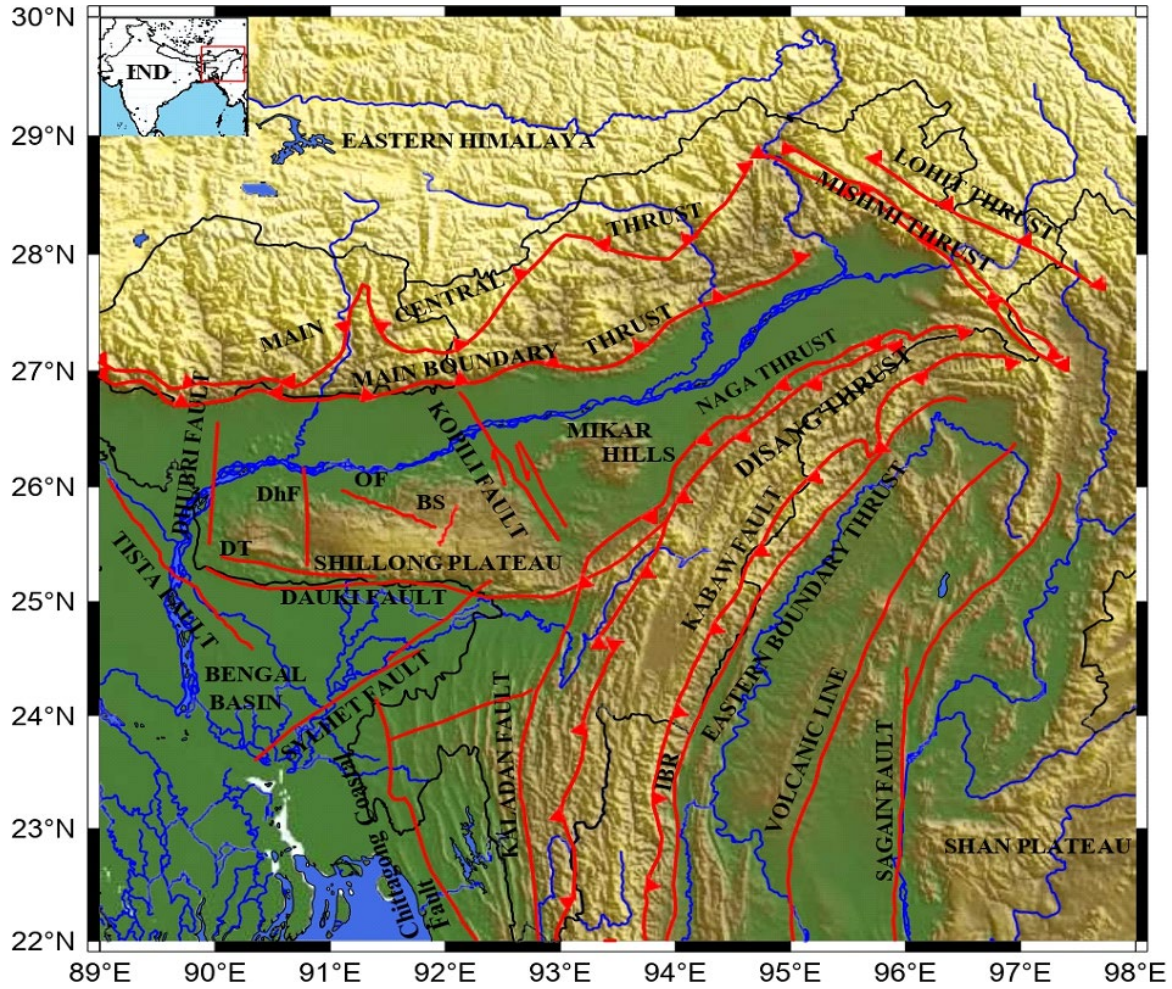


**Figure 1.** The topological plot of the NER of the Indian subcontinent shows various faults and thrusts. The stations set up by the National Center for Seismology (NCS) in this region are shown by yellow for Assam state and red triangles for Meghalaya. The prominent tectonic features in this region include; MCT: Main central thrust, MBT: Main boundary thrust, LH: Lohit thrust, MT: Mishmi thrust, KF: Kabaw fault, SF: Sagaing fault, DF: Dauki fault, SF: Sylhet fault, DT: Dapsi fault, DhF: Dudhoni fault, Dhubri fault, Tista fault, Kaladan Fault, Chittagong Coastal Fault, OF: Oldham fault, BS: Barapani shear zone, NT: Naga-Disang thrust, Kopili fault. The major thrusts located are shown by the teeth lines. Inset map showing the highlighting study region.

Kopili Fault towards the east from the Indo Burmese arc as well as towards the north from the Himalayan arc. As per [Sarma et al., 2018], the seismogenic zone transcends down to  $47 \pm 2$  km for Kopili Fault. However, there is an increase in focal depth as we move from the northern Burma Region to the MCT.

Figure 2 illustrates the current seismicity concerning Kopili Fault and neighboring regions along with prominent tectonic signatures. The yellow stars show the epicentral location of the 28<sup>th</sup> April 2021 earthquake ( $M_w$  6.4).

### 3. Data analysis

The earthquake catalog from 1950 to 2021 of 1398 events has been combined from the international seismological center (ISC) <http://www.isc.ac.uk/> and the United States Geological Survey (USGS) <https://www.usgs.gov/>. This region is bounded by longitude (90°-94°) E and latitude (24°-28°) N. The magnitude of these events ranges from 2-8. The well-known model [Reasenber, 1985] is used for separating the mainshocks or the background earthquakes from after/foreshocks or triggered earthquakes. The conversion relationship has been used to convert various scales i.e  $M_w$ ,  $M_b$ ,  $M_L$ ,  $M_d$ ,  $M_s$  into moment magnitude scale ( $M_w$ ) as suggested by Nath et al. [2017] and Bora [2016]. Before calculating the *b*-value for the study region, another important parameter namely the Magnitude

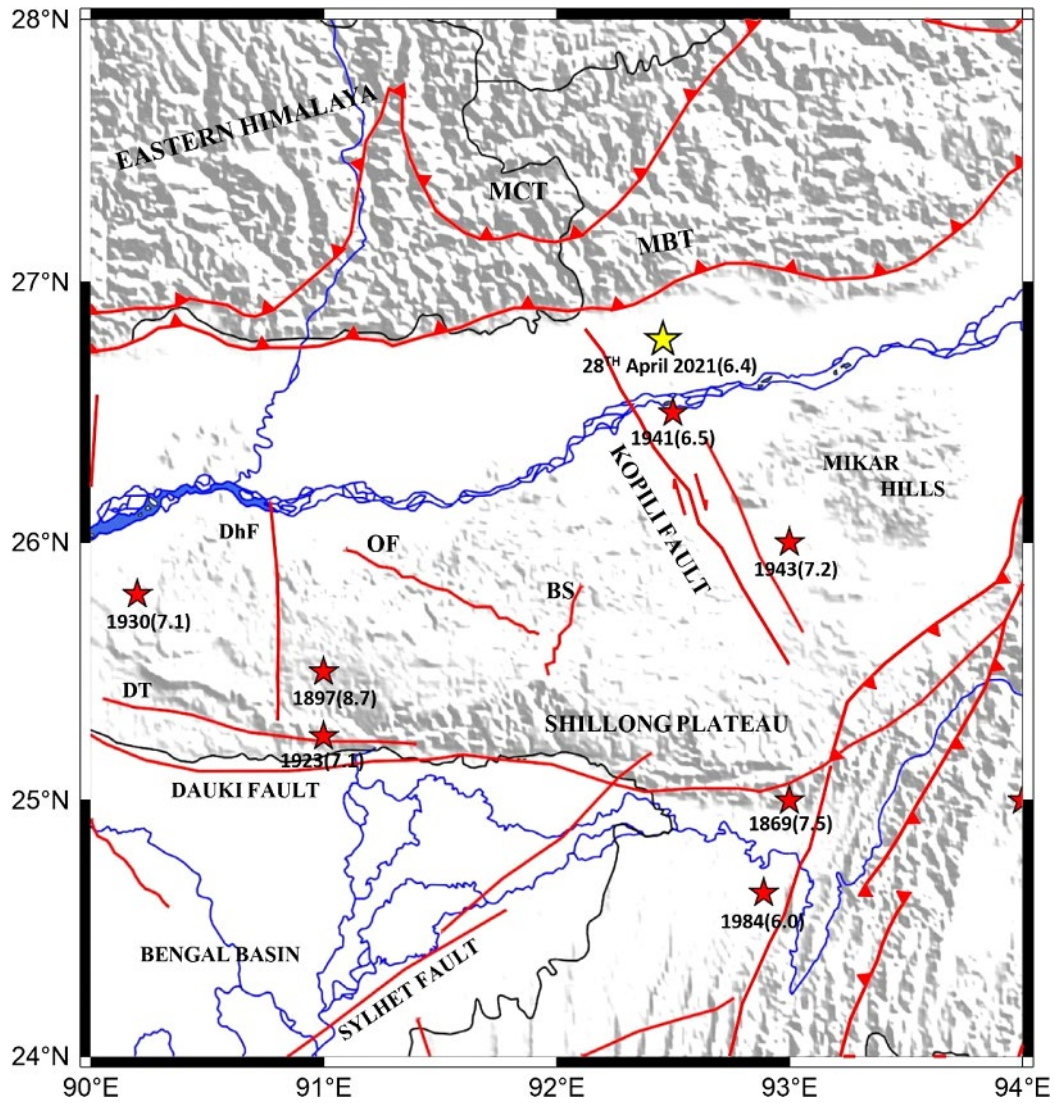


**Figure 2.** The tectonic plot of the study region. the major earthquake events that happened in this region are shown by red stars. The epicentral location 28<sup>th</sup> April 2021 earthquake is shown by the yellow star. MBT: Main boundary thrust, MCT: Main central thrust, OF: Oldham fault, KF: Kabaw fault, NT: Naga-Disang thrust, SF: Sagaing fault, DF: Dauki fault, SF: Sylhet fault, DT: Dapsi fault, DhF: Dudhoni fault, BS: Barapani shear zone, Kopili fault. The thrust lines are shown by the teeth lines.

of completeness ( $M_C$ ) is estimated. This parameter is still considered to be crucial for all seismic-based studies as it helps in optimizing the number of events available and gives a reliable result [Wiemer and Wyss, 2000]. The magnitude of completeness ( $M_C$ ) is the value at which 100% of earthquakes in a space-time volume are detected [Wiemer and Wyss, 2000; Woessner and Wiemer, 2005; Rydelek and Sacks, 1989]. Mousavi [2017a] while mapping seismic moment and  $b$ -value for Iranian plateau established that there happens variation of  $M_C$  due to difference in time of detection by different stations. The recent studies [Das, Wason, and Sharma, 2011; Iwata, 2013; Woessner and Wiemer, 2005] inferred that an increase in the number of earthquake events can lower the  $M_C$  value which applies well here. As the number of stations in this region augments the detection of small earthquake events in this region the  $M_C$  value for this region also decreases over the time. Thus, an accurate estimate of  $M_C$  is important since a very high value will lead to under-sampling, and a very low value considers erroneous seismicity parameter values. In this study, the Maximum-Curvature method has been used to calculate the  $M_c$  for the whole data set [Wiemer and Wyss, 2000] with bootstrapping [Schorlemmer et al., 2003]. The correction factor  $M_c = M_C (\text{MAXC}) + 0.2$  as proposed by Woessner and Wiemer [2005]. For most seismic-based studies, it becomes important to first estimate the value of the magnitude of completeness above which all events are considered for seismic assessment and ultimately this helps to get a reliable result. The completeness magnitude varies as a function of time and space, so particularly

the temporal changes can potentially produce errors in the estimations of seismicity parameters, most commonly the  $b$ -value.

The fluctuation of  $M_c$  as a function of time is depicted using the Zmap tool for seismic data acquired from 1950 to 2021, as shown in Figure 3.

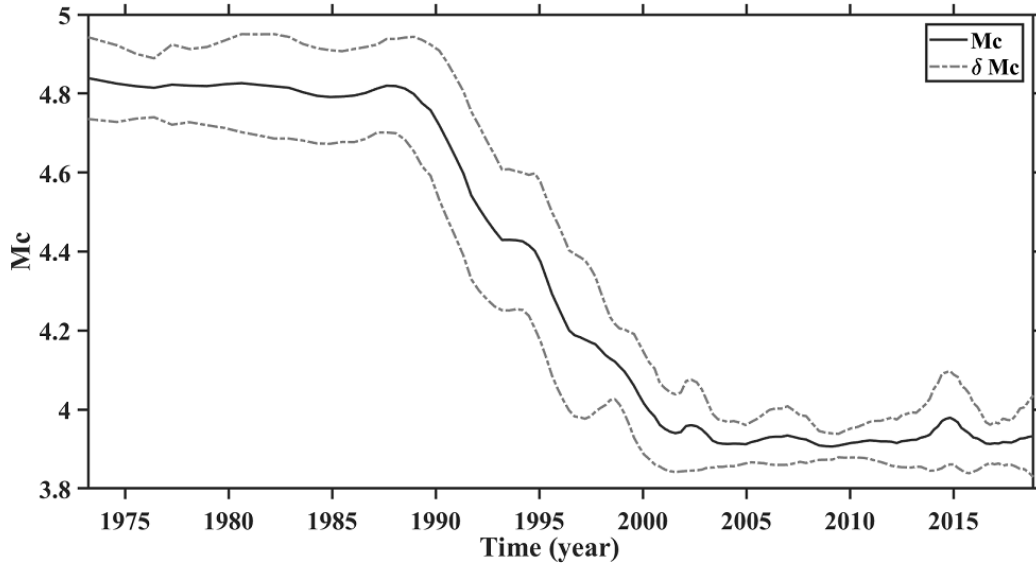


Figure 3. Plot of the magnitude of completeness ( $M_c$ ) variation with time. Standard deviations are shown by dashed lines.

The windowing has been done with 200 samples based on the distribution in the catalog. A closer examination reveals a significant drop in  $M_c$  value after 1993. This could be attributed to a network modification that included the construction of larger receiver sites, as well as severe historical seismic activity in this region, which resulted in a higher number of events being recorded after 1993 as illustrated in Figure 4.

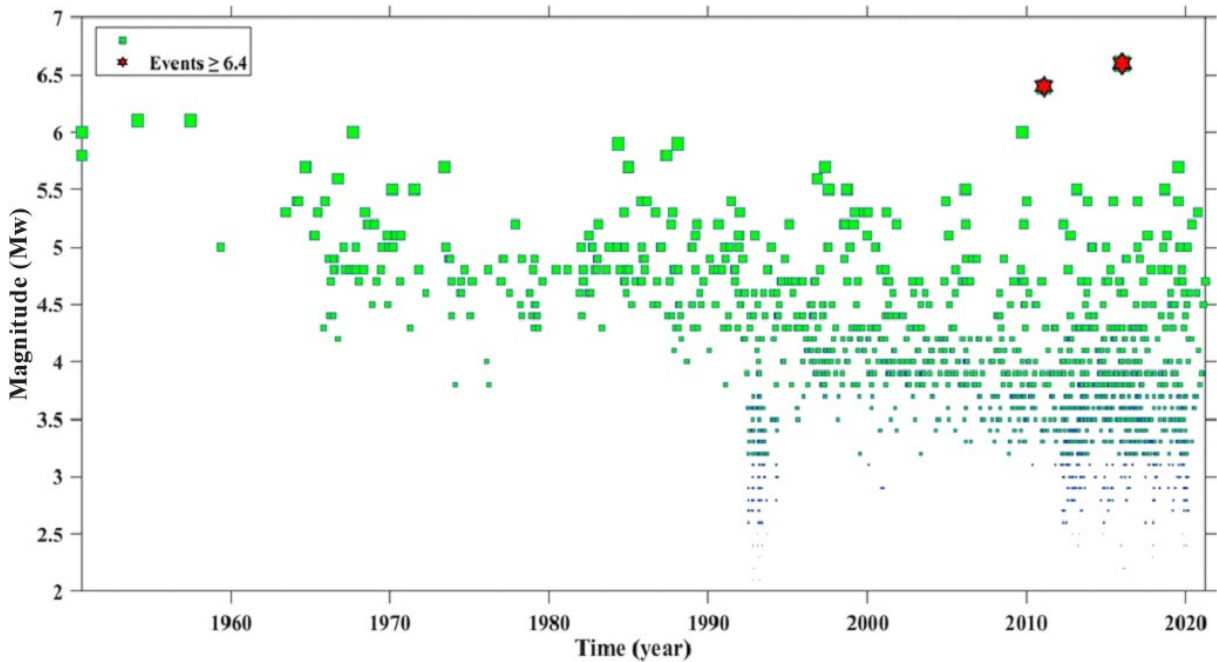


Figure 4. Magnitude ( $M_w$ ) versus time for the research area. The graphic shows a sharp spike in incidents after 1993.

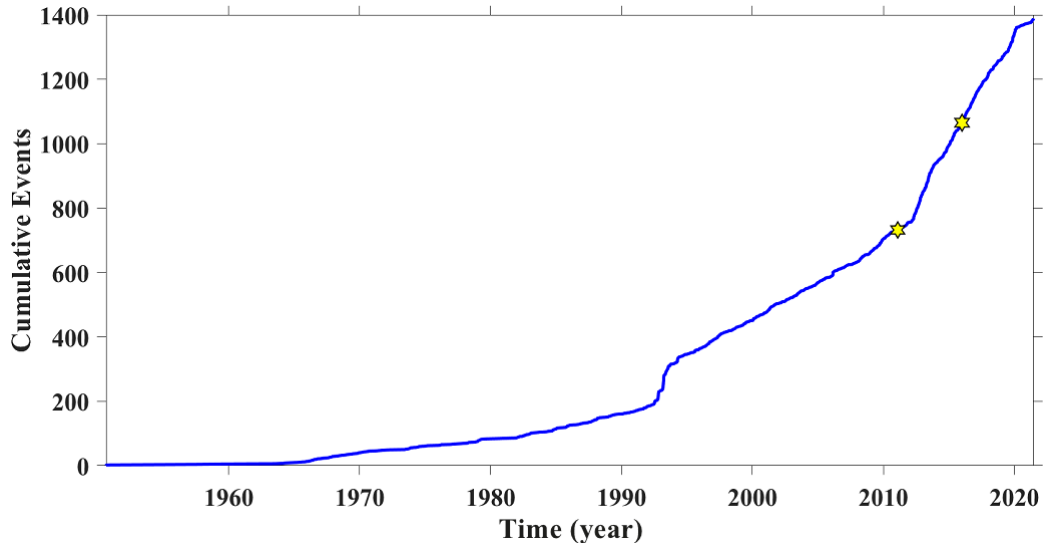


Figure 5. Plot of the cumulative number of earthquake events as a function of time of the region.

The cumulative events' curve shows (Figure 5) an increase in earthquake events observed from 1950 to 2021 and the major events are shown by a star having a magnitude of  $M_w \geq 6.4$ . Considering this, we use this section of the temporal curve to complete  $M_c$  based on the maximum curvature method with subsequent bootstrapping [Wiemer and Wyss, 2000]. Accordingly, the value comes out to be 3.9 with the correction of  $M_c = M_c (MAXC) + 0.2$  as suggested by Woessner and Wiemer [2005] (Figure 6).

Keeping  $M_w \geq M_c$  as the standard, we have chosen 750 events for onward computation of the  $b$ -value. Figure 6 illustrates the G-R power fit law using the maximum likelihood estimate (MLE) [Aki, 1965] to check the linearity of data for the period 1950-2021 with magnitude  $M_w \geq M_c$ . Figure 7 shows the epicentral location of all the seismic events from 1950 to 2021 having  $M_w \geq M_c$ .

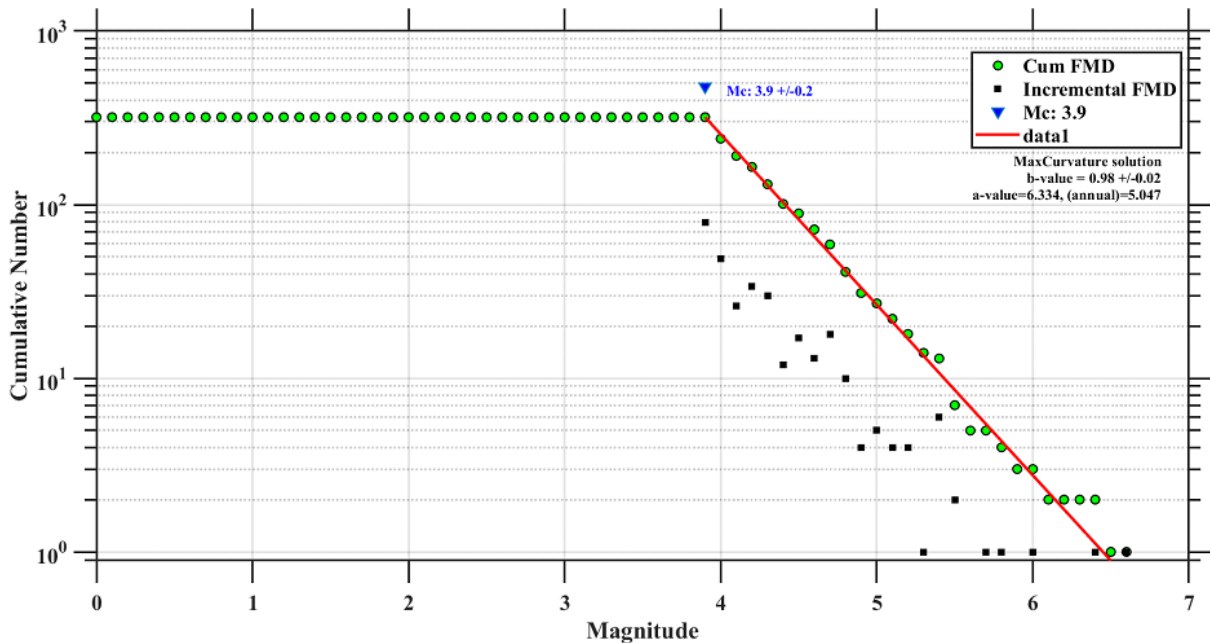
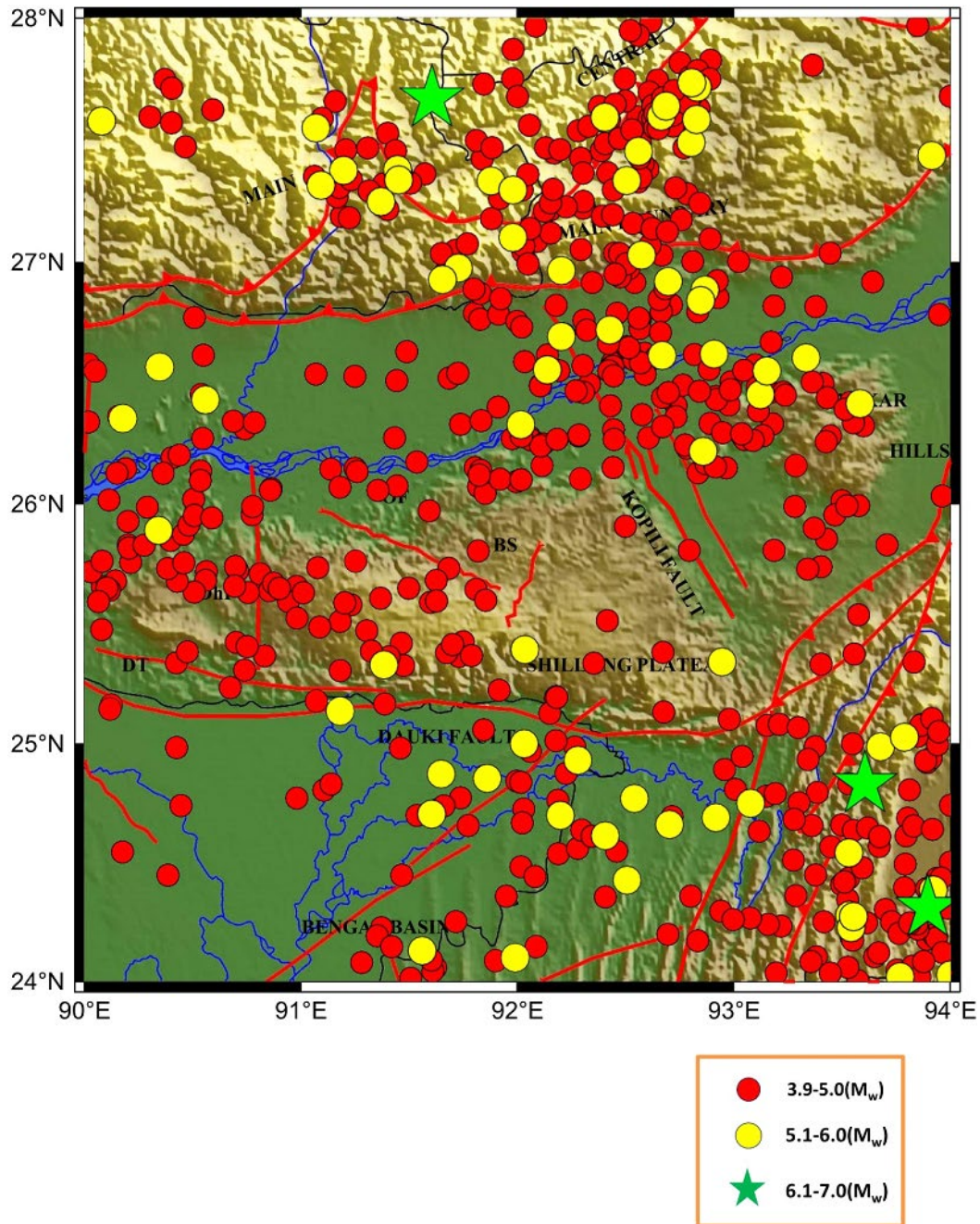


Figure 6. FMD of earthquakes from 2000 to 2021. The straight line is the best fit (Gutenberg and Richter, 1944). The  $M_c$  value shows the magnitude of completeness and the  $b$ -value gives the average  $b$ -value for the complete study region.



**Figure 7.** The epicentral location of all the earthquake events observed in this region (1950-2021) having  $M_w \geq M_c$  is shown in the plot.

#### 4. $b$ -value estimation

Among numerous methods, the two most reliable and well-known methods for the estimation of  $b$ -value are a) *least-square fit method* and b) *maximum likelihood method*. The frequency magnitude distribution follows the principle of Gutenberg and Richter [1944] relation. The present work is based on the method suggested by Aki [1965] i.e. *maximum likelihood method*. This method is best suitable for a small geographical region and time window [Aki, 1965]. The relationship used for the estimation of the  $b$ -value is given by:

$$b = \frac{\log_{10} e}{M - \left( M_c - \frac{\Delta M_{bin}}{2} \right)} \quad (1)$$

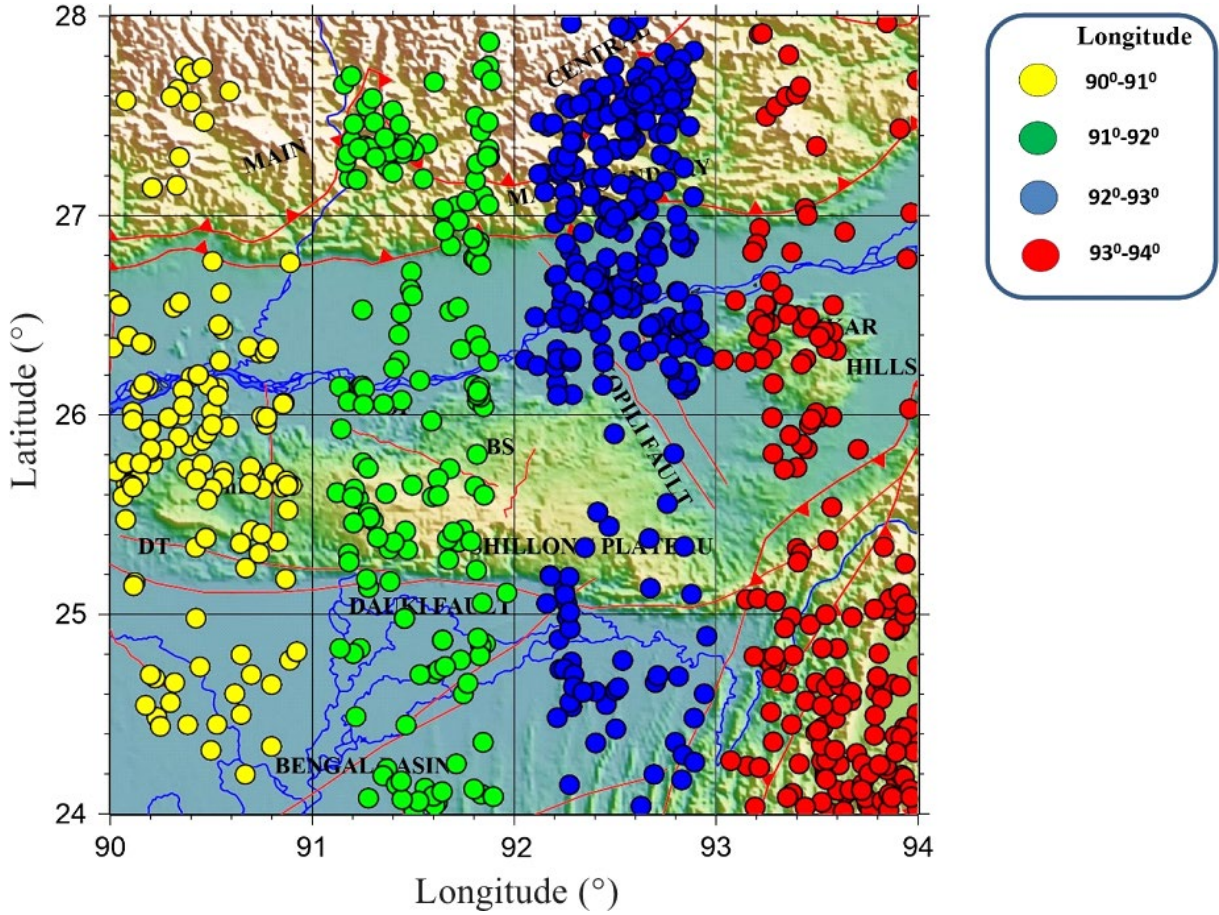


**Figure 8.** The epicentral location of all the earthquake events recorded in the study region from 1950 to 2021 listed in the table1 is shown in the figure. The longitude-wise distribution of these earthquakes is shown by yellow, green, blue, and red marks.

In the above relationship, there are many parameters of significance.  $\bar{M}$  implies average magnitude corresponding to a group of events with magnitude  $M_w$  greater than the magnitude of completeness  $M_C$ . Likewise,  $M_{bin}$  stands for binning width.

Standard deviation  $\delta b$  of the  $b$ -value was given by Aki [1965], and then modified form was given by Shi and Bolt [1982] which is as follows:

$$\delta(b) = 2.30(b^2) \sqrt{\frac{\sum_{i=1}^n \frac{M_i - \bar{M}}{n(n-1)}}{n}} \quad (2)$$

Where 'n' is the total number of events of the given sample.

For the spatial variation of the  $b$ -value, the entire study region is subdivided into 16 equisized grids of  $1^\circ \times 1^\circ$  dimensions. The moving window of  $0.5^\circ \times 0.5^\circ$  has been chosen to retain the natural grid to grid continuity of data points. Several available reports [Kamer, 2014; Kamer and Hiemer, 2013; Mousavi, 2017b; Schorlemmer et al., 2004; Borgohain, Borah, Biswas and Bora, 2018] opined that sufficient data should be present for reliable and better analysis of  $b$ -value; otherwise, less quantity of seismic data may result in undesired and incorrect results. As a result, accuracy, and coverage suffer. Thus, adequate seismic data is required for a better and high-quality outcome. Zmap tool [Wiemer, 2001] is used for the computation of the  $b$ -value for each grid. Table1 depicts the  $b$ -value for each grid and the events that are used for the calculation are shown in Figure 8. The  $b$ -value variation as a function of time is shown in Figure 9. The concept of significant fall in  $b$ -value prior to any main event can be established from the Figure 9.

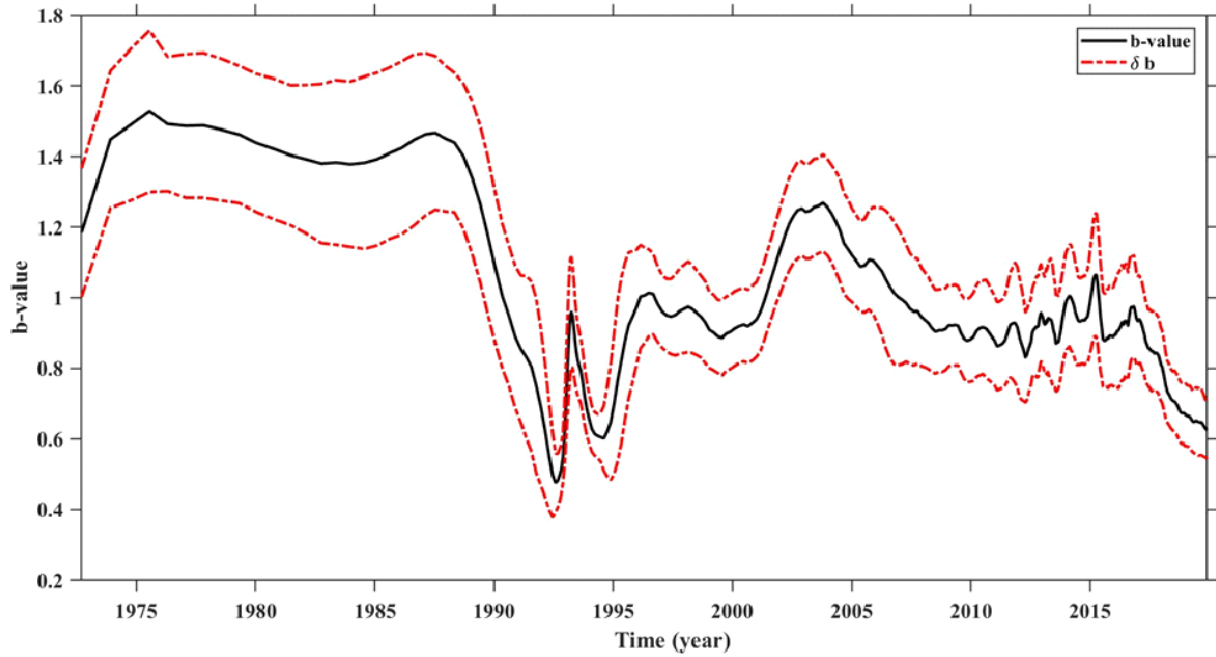


**Figure 9.** The time series projects the variation in  $b$ -value for the study region. A significant fall in  $b$ -value can be traced. The standard deviation is shown by the dashed line.

Longitude (°E)	Latitude (°N)	Nmin	$b$ -value
90-91	24-25	14	0.95
90-91	25-26	63	1.25
90-91	26-27	53	0.94
90-91	27-28	23	0.76
91-92	24-25	49	0.80
91-92	25-26	58	0.84
91-92	26-27	61	0.88
91-92	27-28	60	0.71
92-93	24-25	52	0.68
92-93	25-26	31	0.73
92-93	26-27	139	0.76
92-93	27-28	155	0.72
93-94	24-25	129	0.76
93-94	25-26	49	0.66
93-94	26-27	65	0.83
93-94	27-28	33	0.88

**Table 1.** Spatial variation of  $b$ -value for study region.

The relationship between the  $b$ -value and focal depth is also examined. The next section presents a more in-depth analysis of these results.

## 5. Results and discussions

Furthermore, recent studies [Khan and Chakraborty, 2007; Bhattacharya, Pankaj Majumdar and Kayal, 2002; Khan, Ghosh, Chakraborty, Mukherjee, 2011; Bora, Borah, Mahanta and Borgohain 2018; Mohammed Salih Al-Heety and Mohammad, O. 2021; Tormann, Enescu, Woessner, Wiemer, 2015] inferred that the frequency magnitude distribution factor ( $b$ -value) can vary with several factors including depth, stress accumulation, plate tectonics, and faulting style mechanism.

Due to the subduction of the Indian plate under the Eurasian plate, this region remains under high stress [Sharma and Baruah, 2017]. Figure 10 appraises the variation of  $b$ -values with focal depths of the seismic events. The zmap tool [Wiemer, 2001] has been used to scrutinize the  $b$ -value as a function of depth keeping the minimum magnitude of completeness value fixed. 8 slabs with each slab having a focal depth of 10 km are projected by virtually dividing the area under investigation. The  $b$ -value is plotted against each slab as projected in Figure 10. The lowest  $b$ -value is associated with the upper crust. Similar implications were made by Khan et al. [2011] for the entire NE India and quoted that a low  $b$ -value is observed at a depth range of 25 km to 36 km. The lower  $b$ -value detected at a deeper depth range for the southwest part of the study area may be allied with the rising protuberant of the lithosphere in this region. The low  $b$ -value in the upper crust implies crustal homogeneity. We encounter a low value of 0.66-0.71 confined to the upper crust. The obtained result is plausible with the results that the accumulation of crustal stress in the upper crust is more associated with the in-depth region.

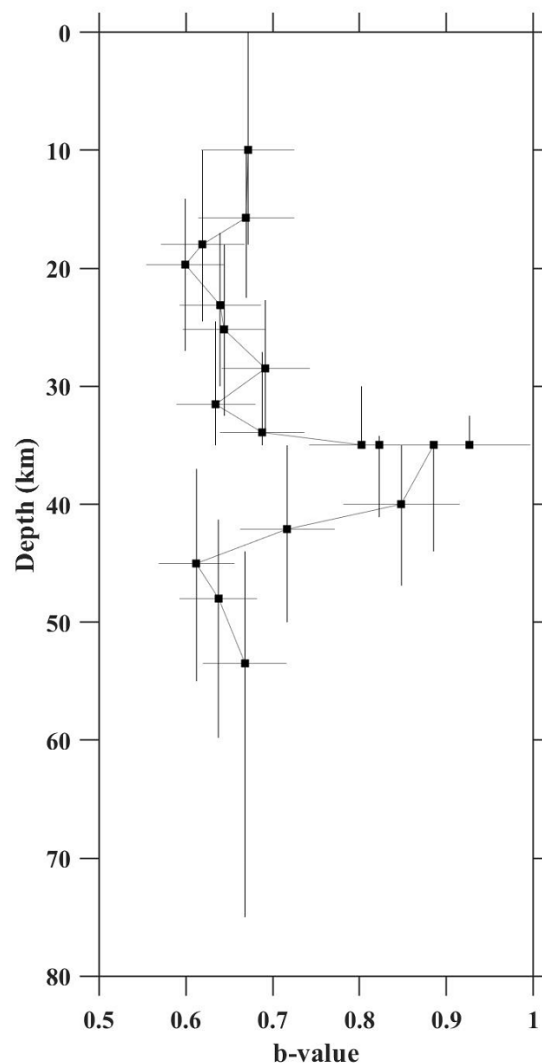


**Figure 10.** Graph showing the variation in frequency magnitude distribution constant ( $b$ -value) concerning depth for the study region.

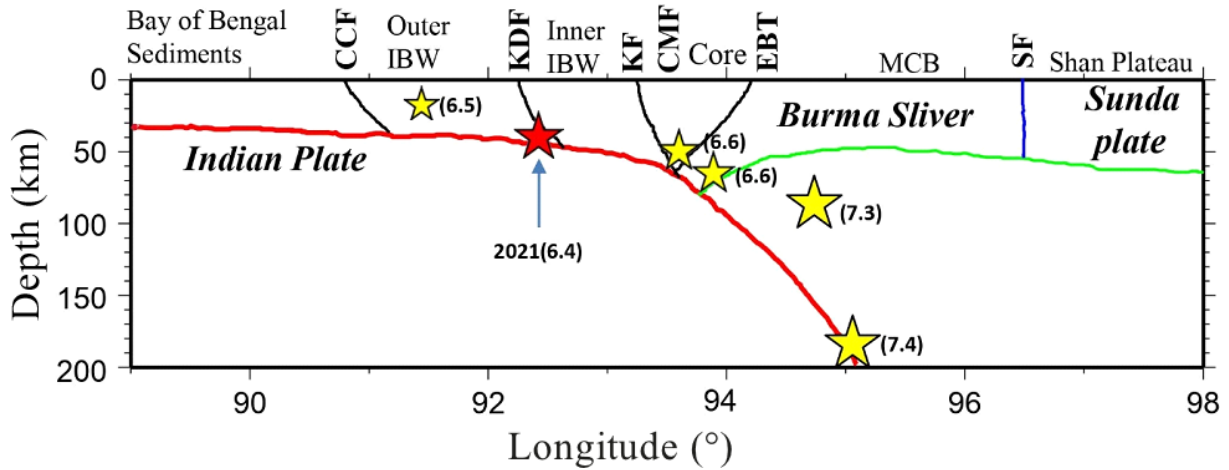


**Figure 11.** The seismotectonic model shows the epicentral location of all the events with magnitude  $M_w \geq 6.5$  observed in this region. The epicentral location of the recent 28<sup>th</sup> April 2021 (6.4) earthquake is shown by a red star.

The interplate model helps us to approximate the location of the 28<sup>th</sup> April 2021 ( $M_w$  6.4) earthquake (Figure 11). It is an interplate earthquake with a reported depth of  $\sim 34$  km [Biswas, 2021]. Mostly interplate earthquakes are observed in this region (Figure 11).

It is stated that crustal homogeneity and high seismic moment are implicated by lower  $b$ -values. Notably, the 2021 event occurred at a depth of 34 km, hinting at the accumulation of stress in the upper crust of the subduction region. As per Huruikawa et al. [2012], subcrustal earthquakes showed depth ranges from 20 to 50 km. Meanwhile, in another study by Montessaro and Kulhaneck, [2003]; higher  $b$ -values were obtained at intermediate depths of 80-100 km beneath Guatemala El-Salvadore as well as for deeper depths of 130-170 km about Nicaragua. A recent study by Bora et al. [2018] reported that the  $b$ -value is  $< 1$  down to 50-55 km depth, and there is a sharp rise in  $b$ -value near 60 km depth in Indo-Burma ranges. In similitude to these observations, the current study attains higher  $b$ -values in intermediate depth (40-45 km) as well as for deeper depth regions. The two studies conducted by Wiemer

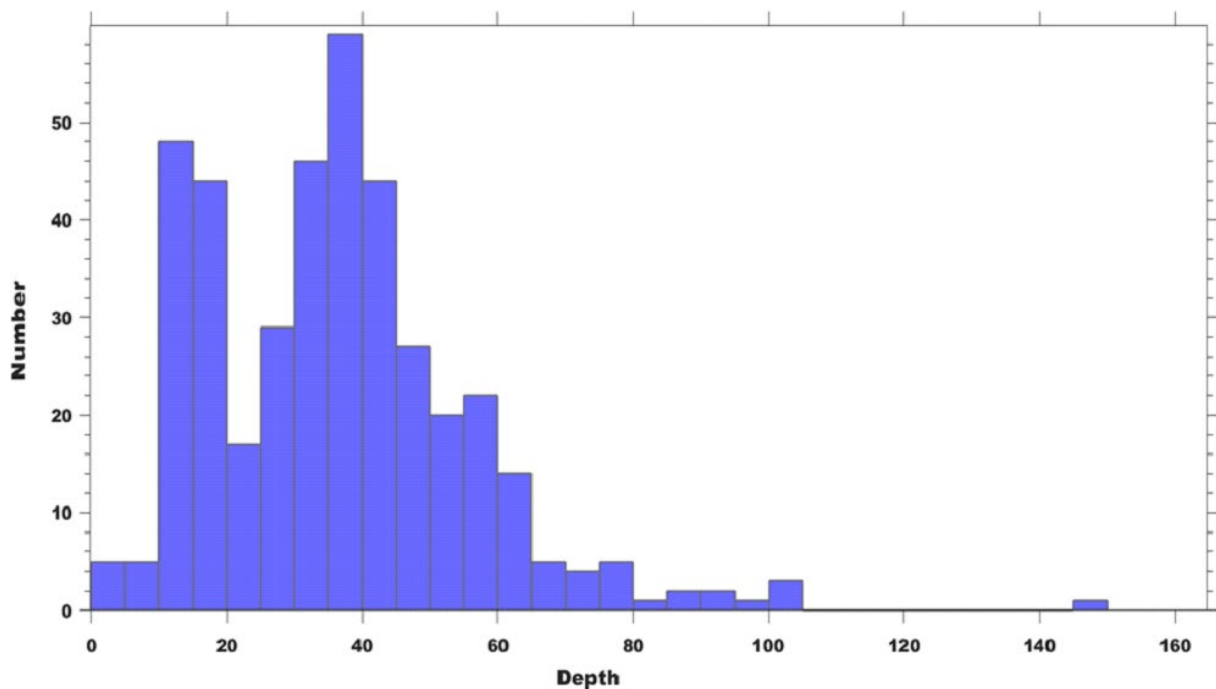


**Figure 12.** Histogram showing depth-wise variation corresponding to chosen 750 events ( $M_w \geq 3.9$ ). The intense seismicity is reported at the focal depth of 30 km to 50 km.

and Benoit [1996] and Wyss et al., [2001] in New Zealand and Alaska respectively report high  $b$ -value anomalies on top of the subducting slabs at depths within 100-150 km depth range. Further, it is observed that the number of events with focal depths greater than 70 km is in a declining trend. Lower tectonic stress at deeper depth with the accompaniment of a high  $b$ -value could be one of the prominent causes of this observation.

The depth histogram as shown in the Figure 12 shows that there is a significant rise in earthquake events for the depth range 30 km to 50 km and the maximum peak is observed at the focal depth of 35 km and the 28<sup>th</sup> April 2021 ( $M_w$  6.4) is also reported at the focal depth of 34 km. The same implications are reported by Khan et al. [2011] that earthquakes events in the study region occurred at the focal depth of 30 km to 50 km.

Likewise, Figure 13 reveals that the number of earthquakes having magnitude  $M_w \sim (4-5)$  is more and only a few events having magnitude  $M_w \geq 5$  are observed in this region.

The spatial variation of the  $b$ -value for the study region is shown in Figure 14. The result shows that the  $b$ -value varies from  $0.66 \pm 0.09$  to  $1.24 \pm 0.11$  for the study region. Khan, Ghosh, Chakraborty and Mukherjee [2011] inferred that the  $b$ -value for northeast India varies from 0.23 to 1.78. Similar implications were made by Bora, Borah, Mahanta and Borgohain [2018] for the indo-Burma region in which the  $b$ -value varies from 0.7 to 1.5.

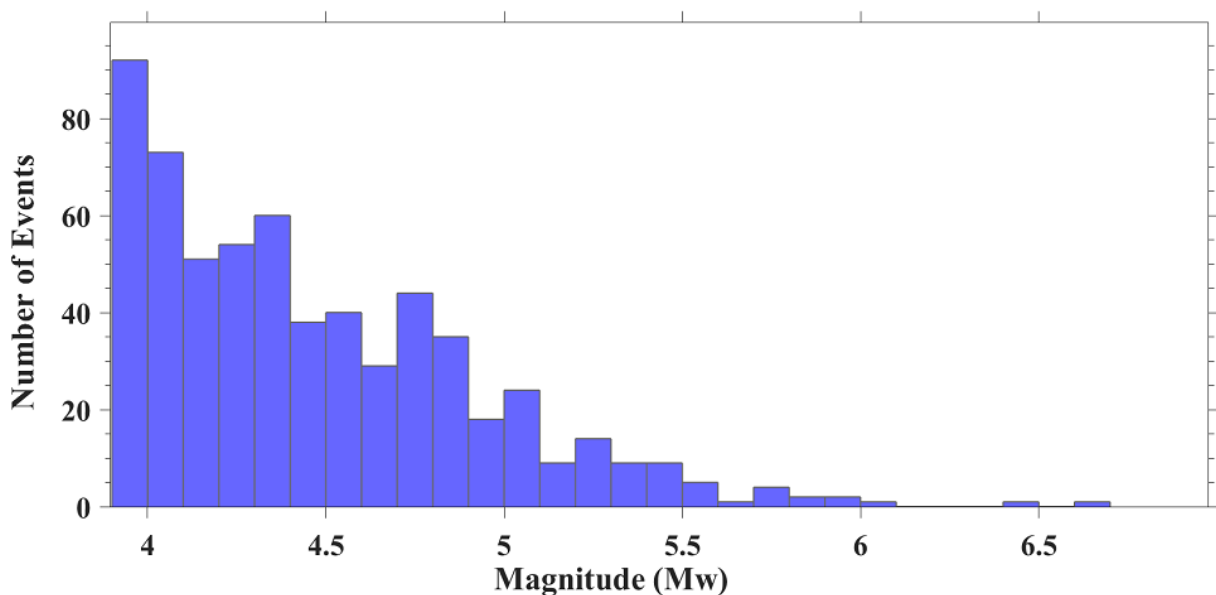


**Figure 13.** Histogram shows the number of earthquakes versus Magnitude for the selected 750 events ( $M_w \geq 3.9$ ). Mostly small magnitude earthquakes with some large magnitude earthquakes are observed in this region.

Thus the observations made from our study show a plausible relationship with already existing results. A recent study [Borgohain, Borah, Biswas and Bora, 2018] reported an intermediate  $b$ -value before the Manipur earthquake (2016). In the present study, low  $b$ -value variation is also observed in the regions between 25-26°N and 93-94°E. These have been suggested to be due to large variations in tectonic stress owing to local variations in the plate tectonic driving forces. Ruff and Kanamori [1980] successfully explain the seismicity and the subduction process by testing the correlation between coupling and other physical features of subduction zones. In contrast, a significant low variation of  $b$ -values is observed (Table 1) around the epicenter of the 28<sup>th</sup> April 2021 ( $M_w$  6.4) Assam earthquake (Lat  $\sim 26.781^\circ$ N, Long  $\sim 92.457^\circ$ E), where the  $b$ -value concentrates around 0.76. The implications made after a global-scale study of  $b$ -value for the large region show  $b$ -value near to unity for any seismically active region but a recent study [Khan, Ghosh, Chakraborty and Mukherjee 2011] shows the variation in  $b$ -value up to 1.78. Our results show good agreement with the already existing studies for the northeast Indian region [eg. Khan, Ghosh, Chakraborty and Mukherjee, 2011; Bora, Borah, Mahanta and Borgohain, 2018]. Certain areas of the study area embody higher stress accumulation relatively. This may be treated as an implication of future impending larger ruptures related to these locations. Since the kopili fault and its neighboring areas are active regions, the current work will prove to be useful for earthquake prediction and seismic hazard assessment.

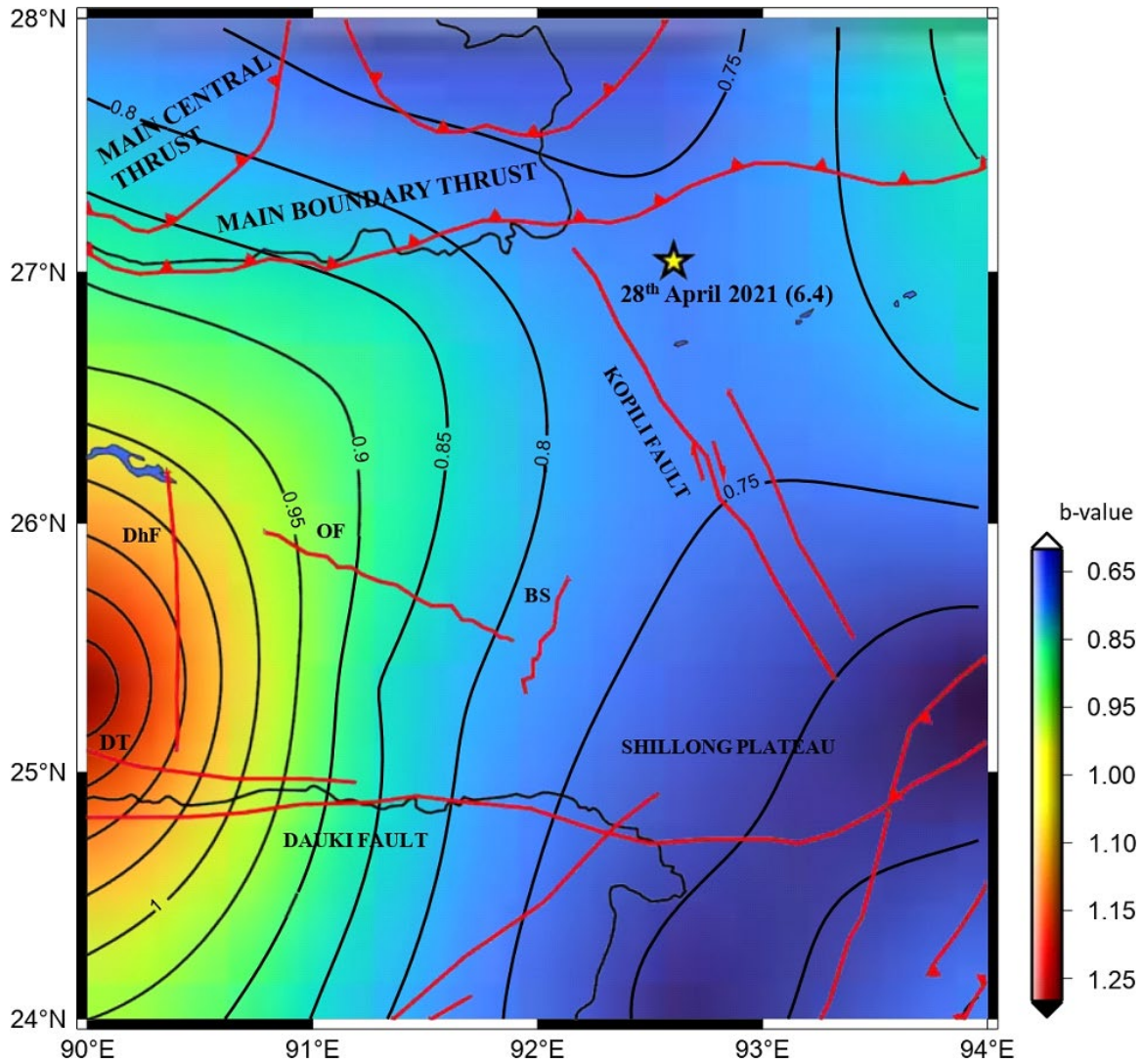


**Figure 14.**  $b$ -value contour map for the study region. The epicentral location of the 24<sup>th</sup> April 2021 earthquake is shown by the yellow star.

## 6. Conclusion

In the current work, a sub sectional approach has been implemented for the formulation of frequency magnitude distribution factor ( $b$ -value) as an earthquake precursor. The entire study region is found to have a  $b$ -value (size distribution) of  $0.98 \pm 0.02$  with a magnitude of completeness of 3.9. The maximum curvature (MAXC) approach is used to calculate the minimal magnitude of completeness ( $M_C$ ). Unreliable results can emerge from an incorrect estimation of the minimum magnitude of completeness. As a result, every precaution was taken to obtain an accurate estimate of the minimum magnitude of completeness. The estimated  $b$ -values are then assessed to build a correlation with the focal depth of the events pertinent to the Kopili fault and its neighboring region of the north-eastern region of India. The earthquake precursor character of change in frequency magnitude distribution ( $b$ -value) can be best described by dividing the whole study region into subsections. Accordingly, 750 well-located events have been utilized to carry out this study. As per findings, the  $b$ -value varies from 0.66 to 1.25 within the region. In addition, a significant low  $b$ -value ( $0.76 \pm 0.03$ ) was observed around the epicentral location of the 28<sup>th</sup> April 2021,  $M_w$  6.4, Assam earthquake; thereby implying accumulation of higher stress. In the upper crust low  $b$ -values (0.66-0.76) are found, which indicate homogeneity and high-stress accumulation. High seismic moment release in the uppermost crust is another reason for the low  $b$ -value. Our study on the Spatio-temporal variation of the  $b$ -value could be used as an earthquake precursor before any mainshock which will ultimately help in earthquake prediction and seismic hazard assessment for this particular region.

**Acknowledgment.** All the maps are drawn using Generic Mapping Tools (GMT) [Wessel et al., 2013] and the graphs are plotted using ZMAP [Wiemer and Wyss, 1997].

## References

- Aki, K. (1965). Maximum likelihood estimate of  $b$  in the formula  $\log N = a - bM$  and its confidence limits, *Boll. Earthq. Res. Inst., Tokyo Univ.*, 43, 237-239.
- Angelier, J. and S. Baruah (2009). Seismotectonics in Northeast India: a Stress Analysis of Focal Mechanism Solutions of Earthquakes and Its Kinematic Implications, *Geophys. J. Int.*, 178,1, 303-326.
- Barman, P., J. D. Ray, A. Kumar, J. D. Chowdhury and K. Mahanta (2016). Estimation of Present-Day Inter-seismic Deformation in Kopili Fault Zone of North-East India Using GPS Measurements, *Geom. Nat. Hazards Risk*, 7, 2, 586-599.
- Bhattacharya, P., R. K. Majumdar and J. Kayal (2002). Fractal Dimension and  $b$ -Value Mapping in Northeast India, *Curr. Sci.*, 82, 1486-1491.
- Bernard, P., H. Lyon-Caen, P. Briole, A. Deschamps, F. Boudin, K. Makropoulos, P. Papadimitriou, F. Lemeille, G. Patau, H. Billiris, D. Paradissis, K. Papazissi, H. Castarède, O. Charade, A. Nercessian, A. Avallone, F. Pacchiani, J. Zahradnik, S. Sacks and A. Linde (2006). Seismicity, Deformation and Seismic Hazard in the Western Rift of Corinth: New Insights from the Corinth Rift Laboratory (CRL), *Tectonophysics*, 426, 1-2, 7-30.
- Bora, D. K., K. Borah, R. Mahanta and J. M. Borgohain (2018). Seismic  $b$ -Values and Its Correlation with Seismic Moment and Bouguer Gravity Anomaly over Indo-Burma Ranges of Northeast India: Tectonic Implications, *Tectonophysics*, 728-729, 130-141.
- Borgohain, J. M., K. Borah, R. Biswas and D. K. Bora (2018). Seismic  $b$ -Value Anomalies Prior to the 3rd January 2016,  $M_w = 6.7$  Manipur Earthquake of Northeast India, *J. Asian Earth Sci.*, 154, 42-48.
- Bora, D. K. (2016). Scaling Relations of Moment Magnitude, Local Magnitude, and Duration Magnitude for Earthquakes Originated in Northeast India, *Earthquake Sci.*, 29, 3, 153-164.
- Bridges, D. L. and S. S. Gao (2006). Spatial Variation of Seismic  $b$ -Values Beneath Makushin Volcano, Unalaska Island, Alaska, *Earth Planet. Sci. Lett.*, 245, 1-2, 408-415.
- Das, R., H. R. Wason and M. L. Sharma (2012). Magnitude Conversion to Unified Moment Magnitude Using Orthogonal Regression Relation, *J. Asian Earth Sci.*, 50, 44-51.
- Das, R., H. R. Wason and M. L. Sharma (2012). Temporal and Spatial Variations in the Magnitude of Completeness for Homogenized Moment Magnitude Catalogue for Northeast India, *J. Earth Syst. Sci.*, 121, 1, 19-28.
- England, P. and R. Bilham (2015). The Shillong Plateau and the Great 1897 Assam Earthquake, *Tectonics*, 34, 9, 1792-1812.
- Gutenberg, B. and C. F. Richter (1944). Frequency of Earthquakes in California, *Bull. Seismol. Soc. Am.*, 34, 4, 185-188.
- Kamer, Y. (2014). Comment on "Systematic Survey of High-Resolution  $b$  Value Imaging Along Californian Faults: Inference on Asperities" by T. Tormann et Al, *J. Geophys. Res.: Solid Earth*, 119, 7, 5830-5833.
- Iwata, T. (2013). Estimation of Completeness Magnitude Considering Daily Variation in Earthquake Detection Capability, *Geophys. J. Int.*, 194, 3, 1909-1919.
- Kamer, Y. and S. Hiemer (2013). Comment on "Analysis of the  $b$ -Values Before and After the 23 October 2011  $M_w$  7.2 Van-Erciș, Turkey, Earthquake.", *Tectonophysics*, 608, 1448-1451.
- Kamer, Y. and S. Hiemer (2015). Data-Driven Spatial  $b$  Value Estimation with Applications to California Seismicity: To  $b$  or Not to  $b$ , *J. Geophys. Res.: Solid Earth*, 120, 7, 5191-5214.
- Kayal, J. (1998). Seismicity of Northeast India and Surroundings – Development over the Past 100 Years, *J. Geophys.*, 19, 9-34.
- Khan, P. K. and P. P. Chakraborty (2007). The Seismic  $b$ -Value and Its Correlation with Bouguer Gravity Anomaly over the Shillong Plateau Area: Tectonic Implications, *J. Asian Earth Sci.*, 29, 1, 136-147.
- Khan, P. K., M. Ghosh, P. P. Chakraborty and D. Mukherjee (2011). Seismic  $b$ -Value and the Assessment of Ambient Stress in Northeast India, *Pure Appl. Geophys.*, 168, 10, 1693-1706.
- Kayal, J.R., S.S. Arefiev, S. Baruah, R. Tatevossian, N. Gogoi, M. Sanoujam, J. L. Gautam, D. Hazarika and D. Borah (2010). The 2009 Bhutan and Assam felt earthquakes ( $M_w$  6.3 and 5.1) at the Kopili fault in the northeast Himalaya region, *Geom. Nat. Hazards Risk, Geom. Nat. Hazards Risk*, 1, 3, 273-281.
- Mahanta, K., J. Chowdhury, A. Kumar, A. Kumar, I. Laskar, S. Laishram and P. Barman (2012). Earthquakes and Crustal Deformation Studies of the Seismically Active Kopili Fault as Well as North East India: A Scientific Field Study Using Global Positioning System (GPS), *Clarion*, 1, 127-132.

- Mogi, K. (1963). Magnitude-Frequency Relation for Elastic Shocks Accompanying Fractures of Various Materials and Some Related Problems in Earthquakes (2nd Paper), Bull. Earthquake Res. Inst. Univ. Tokyo, 40, 4, 831-853.
- Mohammed Salih Al-Heety, E. and O. Mohammad (2021). The Reliance of the Earthquake *b*-Value on Depth and Focal Mechanism, Iraqi Geol. J., 54, 1D, 1-10.
- Mousavi, S. M. (2017a). Mapping Seismic Moment and *b*-Value Within the Continental-Collision Orogenic-Belt Region of the Iranian Plateau, J. Geodyn., 103, 26-41.
- Mousavi, S. M. (2017b). Spatial Variation in the Frequency-Magnitude Distribution of Earthquakes Under the Tectonic Framework in the Middle East, J. Asian Earth Sci., 147, 193-209.
- Nanjo, K. Z., N. Hirata, K. Obara and K. Kasahara (2012). Decade-Scale Decrease in *b* Value Prior to the M9-Class 2011 Tohoku and 2004 Sumatra Quakes, Geophys. Res. Lett., 39, 20, L20304.
- Nuannin, P., O. Kulhanek and L. Persson (2005). Spatial and Temporal *b* Value Anomalies Preceding the Devastating off Coast of NW Sumatra Earthquake of December 26, 2004, Geophys. Res. Lett., 32, 11.
- Nath, S. K., S. Mandal, M. D. Adhikari and S. K. Maiti (2017). A Unified Earthquake Catalogue for South Asia Covering the Period 1900-2014, Nat. Hazards, 85, 3, 1787-1810.
- Roy, A. B. and R. Purohit (2018). Chapter 17, The Himalayas: Evolution Through Collision, A. B. Roy and R. B. T.-I. S. Purohit (Editor), Elsevier 311-327.
- Ruff, L. and H. Kanamori (1980). Seismicity and the Subduction Process, Phys. Earth Planet. Inter., 23, 3, 240-252.
- Rydelek, P. A. and I. S. Sacks (1989). Testing the Completeness of Earthquake Catalogs and the Hypothesis of Self-Similarity, Nature, 337, 6204, 251-253.
- Reasenberg, P. (1985). Second-Order Moment of Central California Seismicity, 1969-1982, J. Geophys. Res., 90, B7, 5479-5495.
- Biswas, R. (2021). A brief review of the recent Assam Earthquake 5, 1-2.
- Schorlemmer, D., S. Wiemer and M. Wyss (2004). Earthquake Statistics at Parkfield: 1. Stationarity of *b* Values, J. Geophys. Res.: Solid Earth, 109, (B12).
- Schorlemmer, D., S. Wiemer and M. Wyss (2005). Variations in Earthquake-Size Distribution Across Different Stress Regimes, Nature, 437, 7058, 539-542.
- Sharma, S. and S. Baruah (2017). Modelling of the Kopili Fault Based on Slip Rate, Moment Rate and Seismic Activity in Mikir Hills Plateau of Northeastern India, Geom. Nat. Hazards Risk 8, 2, 1157-1172.
- Sharma, S., J. Sarma and S. Baruah (2018). Dynamics of Mikir Hills Plateau and Its Vicinity: Inferences on Kopili and Bomdila Faults in Northeastern India Through Seismotectonics, Gravity and Magnetic Anomalies, Ann. Geophys., 61, 3.
- Sorbi, M. R., F. Nilfouroushan and A. Zamani (2012). Seismicity Patterns Associated with the September 10th, 2008 Qeshm Earthquake, South Iran, Int. J. Earth Sci., 101, 8, 2215-2223.
- Tormann, T., B. Enescu, J. Woessner and S. Wiemer (2015). Randomness of megathrust earthquakes implied by rapid stress recovery after the Japan earthquake, Nat. Geosci., 8, 2, 152-158.
- Shi, Y. and B. A. Bolt (1982). The Standard Error of the Magnitude-Frequency *b* Value, Bull. Seismol. Soc. Am., 72, 5, 1677-1687.
- White, B. J. P., R. B. Smith, S. Husen, J. M. Farrell and I. Wong (2009). Seismicity and Earthquake Hazard Analysis of the Teton-Yellowstone Region, Wyoming, J. Volcanol. Geotherm. Res., 188, 1-3, 277-296.
- Wiemer, S. and J. P. Benoit (1996). Mapping the *b*-value Anomaly at 100 km Depth in the Alaska and New Zealand Subduction Zones, Geophys. Res. Lett., 23, 13, 1557-1560.
- Wiemer, S. and M. Wyss (2000). Minimum Magnitude of Completeness in Earthquake Catalogs: Examples from Alaska, the Western United States, and Japan, Bull. Seismol. Soc. Am., 90, 4, 859-869.
- Woessner, J. and S. Wiemer (2005). Assessing the Quality of Earthquake Catalogues: Estimating the Magnitude of Completeness and Its Uncertainty, Bull. Seismol. Soc. Am., 95, 2, 684-698.
- Wyss, M., S. Wiemer and F. Zúñiga (2001). ZMAP a Tool for Analyses of Seismicity Patterns. Typical Applications and Uses: A Cookbook by M. Wyss, S. Wiemer and R. Zúñiga.

\*CORRESPONDING AUTHOR: Rajib BISWAS,

Applied Geophysics Lab, Department of Physics, Tezpur University, Tezpur-784028, India  
e-mail: rajib@tezu.ernet.in